Materials Letters 215 (2018) 27–30

Contents lists available at ScienceDirect

Materials Letters

journal homepage: www.elsevier.com/locate/mlblue

Fe-doped brushite bone cements with antibacterial property

Guangda Li [a], Nan Zhang [a], Santuan Zhao [b,*], Kaili Zhang [a], Xiaoyu Li [a], Aihua Jing [a], Xinping Liu [c], Tian Zhang [a]

[a] College of Medical Technology and Engineering, Henan University of Science and Technology, Luo Yang 471023, Henan, PR China
[b] College of Material Science and Engineering, Henan University of Science and Technology, Luo Yang 471023, Henan, PR China
[c] Key Laboratory of Biologic Resources Protection and Utilization of Hubei Province (Hubei Institute for Nationalities) and Department of Chemistry, Enshi 445000, Hubei, PR China

ARTICLE INFO

Article history:
Received 18 July 2017
Received in revised form 3 October 2017
Accepted 10 December 2017
Available online 11 December 2017

Keywords:
Biomaterials
Bioceramics
Brushite bone cement
Iron
Antibacterial

ABSTRACT

In present research, Fe-doped brushite bone cements were synthesized. The setting time, microstructure and antibacterial property of samples were investigated. The results showed that the setting time of cements was retarded to about 20 min and 123 min, respectively, as iron doping content increasing from 1 mol% to 5 mol% in β-TCP powder. Moreover, Fe-doped cements had much bigger crystal particles and calcium iron phosphate was identified in them. Furthermore, Fe-doped cements performed well in inhibiting the growth of *Staphylococcus aureus* and *Pseudomonas aeruginosa*, and larger inhibition halo was obtained with more iron content. Nevertheless, the Fe-loaded cements were not so sensitive to *Escherichia coli* as to the other two bacteria.

1. Introduction

Brushite bone cement (BC) attracts much attention as bone replacement materials due to their excellent degradability and long-term inclusion in bone remodeling [1]. In order to cope with inflammation and protect the surrounding tissue during implantation, great efforts have been put on developing BC with local antibacterial property [2]. One approach is to load various regimes of antibiotics on BC [1]. Nevertheless, the use of antibiotics is costly and is linked with the global problem of rising immunity of pathogens to traditional antibiotic therapies [3]. Thus, the incorporation of antibacterial cations, mainly Ag^+ and Cu^{2+}, into BC has been proposed. Ewald et al. proved that Ag-doped BC had antimicrobial activity comparable to antibiotic treatment [4]. Ag, however, is not a necessary element for human. The possible side effects of resistance, allergy, or skin discoloration are worrying [5]. Dominika et al. revealed that the copper-doped BC exhibited antibacterial effect against gram-negative bacteria but appeared to increase the proliferation of gram-positive S. aureus [3]. Though copper is an essential trace element in human body, the requirement is in very small amount and dose control must be strictly careful [6].

Is there any other cation for choice? Iron (Fe) is an essential element that plays a critical role in the normal growth and metabolism of hard tissues. Human body demands a much higher amount of iron than other trace elements [6]. Moreover, the addition of iron to apatite bone cements can not only improve the mechanical strength and cell affinity in vitro [7,8], but also lead to firm bone binding in vivo [9]. Recently, Fe-doped perovskite particles and Fe^0 nanoparticles were proved to be antibacterial [10,11]. To our knowledge, there was no literature reported about evaluating the antibacterial behaviour of iron-doped BC. In present study, Fe-doped brushite cements were synthesized and their bactericidal activity against *Staphylococcus aureus*, *Pseudomonas aeruginosa* and *Escherichia coli* was tested using agar diffusion assay.

2. Materials and methods

All chemicals used were of analytical grade (bought from Kemiou Lt. Co, China). The water used is deionized water.

2.1. Preparation of β-tricalcium phosphate (β-TCP) and Fe-substituted β-TCP (Fe-β-TCP)

The β-TCP and Fe-β-TCP powders were prepared by aqueous precipitation method modified from other research [12]. Briefly, mixture solution of $Ca(NO_3)_2$ and $Fe(NO_3)_3$ (Fe/(Fe + Ca) = 0, 1, 3, 5 mol%) was prepared with the total metal cation concentration of 0.1 mol/L. Then certain amount of $(NH_4)_2HPO_4$ solution (0.1 M) was added to the mixture solution, assuming that all the products were orthophosphate. During the 4 h long reaction process, the pH value was kept at around 7 by dropwise addition of $NH_3{\cdot}H_2O$ under

* Corresponding author.
E-mail address: stzhao@haust.edu.cn (S. Zhao).

https://doi.org/10.1016/j.matlet.2017.12.054

stirring, and the temperature was controlled using ice water. The as obtained suspension liquid was aged for 36 h at 40 °C. The precipitate was vacuum filtrated, dried at 110 °C and then buried in carbon and heated for 2 h at 1000 °C. The sintered powder was crushed and 200-mesh sieved.

2.2. Preparation of cement

β-TCP or Fe-β-TCP (1.2 g) was mixed with monocalcium phosphate hydrate (MCPM) (1.0 g, 200-mesh sieved) as cement powder. The cement liquid was 0.5 M citric acid solution with the addition of 1 wt% chitosan. The liquid to powder ratio was 0.33 ml/g. After mixing, the cement paste was immediately placed into moulds to ensure standardized shapes. The cement disks were removed from the moulds after setting. And cement was named as Fe-0, Fe-1, Fe-3 and Fe-5 according to the Fe doping concentration of 0%,1%,3% and 5%, respectively.

2.3. Cement characterization

The setting time of cements (n = 5, Φ 8 × 3 mm) was determined using the method as other research [13]. The cement was considered as setting when a Vicat needle with a tip diameter of 1 mm and load of 400 g failed to make a perceptible circular indentation on the surface. After curing for 72 h, the surface morphology and structure of the cements were analyzed by SEM (Tescan Vega), X-ray diffraction (XRD, PANalytical X'Pert-PRO MPD) and Fourier transform infrared spectroscopy (FT-IR, Thermo Fisher Nicolet IS10), respectively.

2.4. Antibacterial experiments

For sterilizing, the cement discs (Φ 5 × 2 mm) were first soaked in 75% alcohol for 30 min, and then placed under UV light for 3 h and dried under 37 °C. The antibacterial properties were evaluated by inhibition halo test in accordance with other research [14] using *Staphylococcus aureus strain* (ATCC 25923), *Escherichia coli strain* (ATCC 35218) and *Pseudomonas aeruginosa strain* (ATCC 27853). A 100 μl of bacterial suspension with the concentration about 2 × 10^8 $CFUml^{-1}$ were seeded on the Mueller Hinton agar plates by a spreader. Each sample was placed in plates and the plates were cultured for 24 h at 37 °C. All the cements for this assay were analyzed in triplicates, and callipers were used to measure zones of inhibition.

3. Results and discussion

Fig. 1 displays the setting time and morphology of cements. The cement setting process was significantly retarded by Fe addition. Sample Fe-5 had a setting time as long as about 123 min. Meanwhile, the crystal particles were observed to be much bigger in Fe-loaded samples. The XRD results (Fig. 2a) revealed that all cements set into brushite (JCPDS 09-0077). But the brushite peaks' intensity dropped in Fe-loaded samples, especially remarkable for Fe-5. Moreover, calcium iron phosphate ($Ca_{19}Fe_2(PO_4)_{14}$, JCPDS 49-1223) and unreacted MCPM (JCPDS 09-0347) were detected, and the content of these two compounds increased with increasing Fe content. The FT-IR spectra (Fig. 2b) further confirms the XRD results. The sharp bands characterizing the HPO_4 group at about 1140, 1064, 987, 873 cm^{-1} (P-O stretching), 788 cm^{-1} (H-out-of-plane bending), 579 and 526 cm^{-1} (O-P-O bending) was detected in Fe-0 [15]. While, all these bands shifted to higher wave number and the intensity dramatically went down for sample Fe-5, which demonstrated less brushite and large lattice deformation resulting from the Fe addition. Moreover, several new bands, namely at

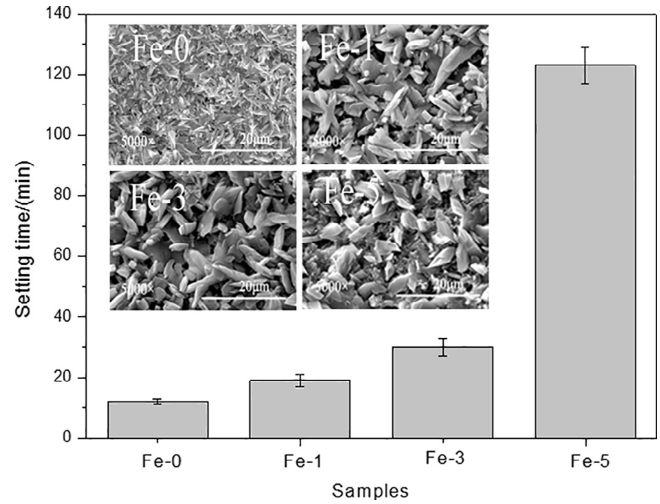

Fig. 1. Setting time and surface morphology of cements.

a

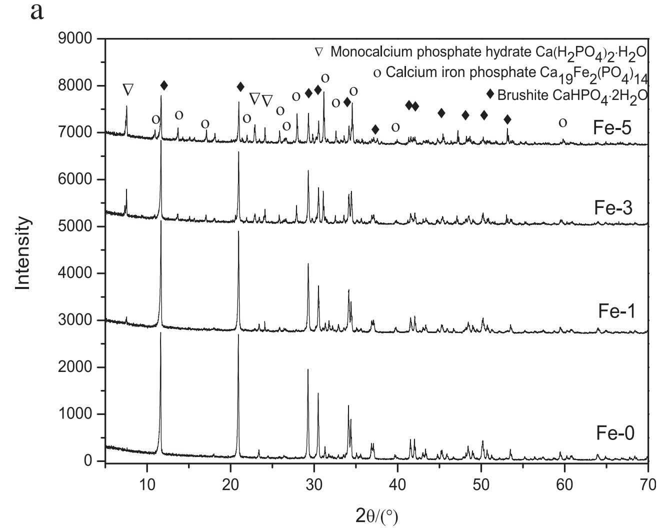

b

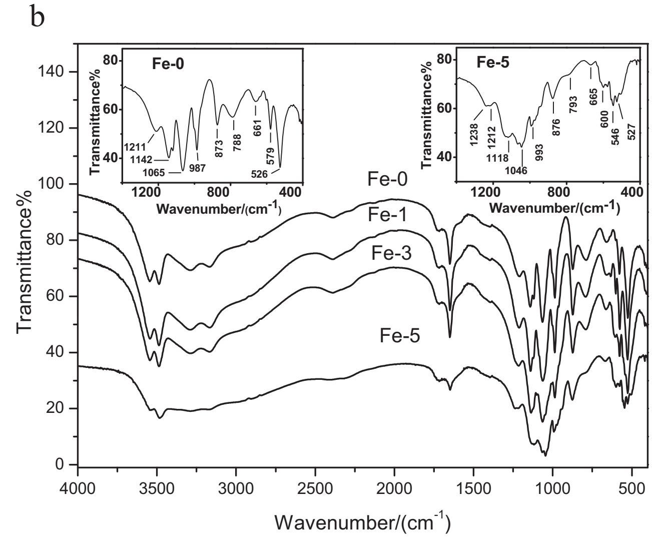

Fig. 2. Microstructure of cements: (a) XRD patterns, (b) FT-IR spectra.